

A study of the role of Lyman β fluorescence on OI line strengths in Be stars

Blesson Mathew¹, D. P. K. Banerjee¹, A. Subramaniam² and N. M. Ashok¹

¹*Astronomy and Astrophysics Division, Physical Research Laboratory, Navrangapura, Ahmedabad - 380 009, Gujarat, India*

²*Indian Institute of Astrophysics, Bangalore - 560 034, India*

blesson@prl.res.in

ABSTRACT

The possibility of the Ly β fluorescence mechanism being operational in classical Be stars and thereby contributing to the strength of the OI 8446 Å line has been recognized for long. However this supposition needs to be quantified by comparing observed and predicted OI line ratios. In the present work, optical and near-infrared spectra of classical Be stars are presented. We analyse the observed strengths of the OI 7774, 8446, 11287 and 13165 Å lines which have been theoretically proposed as diagnostics for identifying the excitation mechanism. We have considered and examined the effects of Ly β fluorescence, collisional excitation, recombination and continuum fluorescence on these OI line strengths. From our analysis it appears that the Ly β fluorescence process is indeed operative in Be stars.

Subject headings: stars: emission-line, Be — techniques: spectroscopic — atomic processes — infrared: stars — (stars:) circumstellar matter

1. Introduction

Classical Be (CBe) stars are non-supergiant B-type stars whose spectrum, to enable a definition in a broad sense, show or have shown Balmer lines in emission at some stage (Collins 1987). These and other emission lines are formed in a circumstellar gaseous decretion disk which is also the source for a significant infrared continuum excess arising from free-free and bound-free emission. It has been considered for long that the disk is formed as the outcome of Be stars being fast rotators. However, whether formation of a geometrically thin disk can be caused solely by rotation is not as yet a resolved issue (for e.g., see the review

by Porter & Rivinius (2003)). Recent studies suggest that CBe stars are rotating close to their critical velocities and other mechanisms like non-radial pulsations, magnetic fields or binarity can possibly contribute to explaining the Be phenomenon (Meilland et al. 2012).

The dynamics and nature of the circumstellar disk can be understood in a better manner from spectroscopic observations. One of the initial efforts in this direction is by Slettebak (1982) who estimated the spectral types and rotational velocities of 183 Oe, Be, A-F type shell stars brighter than 6 magnitude. Subsequently, several other detailed spectroscopic surveys have been done both in the optical (for example Andrillat & Fehrenbach (1982), Andrillat, Jaschek & Jaschek (1988), Dachs et al. (1986), Dachs, Hummel & Hanuschik (1992), Banerjee, Rawat & Janardhan (2000), Hanuschik (1986), Hanuschik (1987)) and in the near-infrared (for example Clark & Steele (2000), Steele & Clark (2001)) to understand the behavior and temporal evolution of different lines and in general to understand the Be phenomenon. Our present study focuses on studying the strengths of certain OI lines that are commonly seen in the optical and near-infrared spectra of CBe stars viz. the OI 7774, 8446, 11287 and 13165 Å lines. The motivation for studying these lines is discussed below in greater detail. Our optical sample of CBe stars is drawn from earlier studies of Mathew, Subramaniam & Bhatt (2008) and Mathew & Subramaniam (2011) wherein we had surveyed, identified and obtained spectra of 150 CBe stars in selected open clusters.

Among the OI lines one may begin by considering OI λ 8446 which is present in emission in the spectra of several astrophysical sources viz. emission-line stars, HII regions, planetary nebulae, novae, Seyfert galaxies and QSOs. It is an interesting line because there has been considerable discussion in the literature on the possible mechanisms which excite it. It is generally accepted that $\text{Ly}\beta$ fluorescence, apart from other mechanisms like collisional excitation, recombination and continuum fluorescence, can greatly contribute to the observed strength of the line. The $\text{Ly}\beta$ fluorescence mechanism was proposed by Bowen (1947) wherein due to the near coincidence of wavelengths, Hydrogen $\text{Ly}\beta$ photons at 1025.72 Å can pump the OI ground state resonance line at 1025.77 Å thereby populating the OI $3d^3D^0$ level. The subsequent downward cascade produces the 11287, 8446 and 1304 Å lines in emission. This was referred to as a PAR process (photoexcitation by accidental resonance) by Bhatia & Kastner (1995) (hereafter BK95) who constructed a detailed model for neutral oxygen and computed expected strengths of the various OI lines when collisional excitation was the sole excitation mechanism (BK95) and followed it with a second study in which the PAR process was also considered (Kastner & Bhatia (1995), hereafter KB95). In the present study, we have used the results from these two studies to understand the neutral OI spectrum of CBe stars and discriminate whether the PAR process is indeed responsible for the observed strength of the 8446 Å line in these stars. That the $\text{Ly}\beta$ fluorescence process could be operating in CBe stars has been suggested since long. For example as early as 1951, Slettebak (1951) in a

survey of 25 CBe stars pointed out the anomalies in the strengths of the 7774 Å and 8446 Å lines with the well known tendency of $\lambda 8446$ to go into emission more readily than $\lambda 7774$. This was attributed to the $\text{Ly}\beta$ process increasing the strength of the 8446 Å line. A similar conclusion was reached by Burbidge (1952) while studying the CBe star χ Oph. However, as of today, observational strengths of the OI lines in Be stars do not appear to have been compared in a comprehensive manner with the detailed theoretical calculations, such as those of BK95 and KB95, to establish whether the $\text{Ly}\beta$ fluorescence process really affects the neutral OI spectrum. In the present work, we study the behavior of the OI 7774, 8446 Å lines in the optical and the OI 11287 and 13165 Å lines in the near infrared and show that there is convincing evidence indicating that the $\text{Ly}\beta$ fluorescence process is indeed operational in CBe stars.

2. Observations & Analysis

Our optical sample of CBe stars is drawn from the study of Mathew, Subramaniam & Bhatt (2008) who performed a survey to identify CBe stars in 207 open clusters using slitless spectroscopy. The spectroscopy of 150 CBe stars in 39 open clusters in the wavelength range 3800 – 9000 Å is presented in Mathew & Subramaniam (2011) – the optical spectra analysed here are from this study. Briefly, these spectroscopic observations were done using the HFOSC imager-spectrograph instrument available with the 2.0m Himalayan Chandra Telescope (HCT), located at Hanle, India. The CCD used for imaging is a 2 K \times 4 K CCD, with a pixel size of 15 μ and an image scale of 0.297 arcsec/pixel. The spectra of CBe stars were taken at an effective resolution of 7 Å around the $\text{H}\alpha$ line. More details on the observations are presented in Mathew & Subramaniam (2011) and details on the HFOSC are available at the website www.iiap.res.in. All the observed spectra were wavelength calibrated and corrected for instrument sensitivity using the Image Reduction and Analysis Facility (IRAF) tasks. IRAF was also used for all further data reduction and analysis including measurements of the equivalent widths (W) of the spectral lines - the typical error in the measurement of W values is around 10%.

The J band spectra were obtained at a resolution of ~ 1000 using the Near-Infrared Imager/Spectrometer with a 256 \times 256 HgCdTe NICMOS3 array, mounted on the 1.2m Mt. Abu telescope. For each object a set of two spectra were taken with the star dithered to two different positions along the 1 arcsec wide slit. Spectral calibration was done using OH airglow and telluric lines which register with the stellar spectrum. Following the standard practice used in the near-IR, the telluric lines present in the object spectra were removed through a rationing process, in which the object spectrum is divided by the standard star

spectrum. The standard star was always observed at similar airmass as the object and prior to rationing the hydrogen lines in its spectrum were removed by interpolation. The rationed spectra were finally multiplied by a blackbody spectrum, corresponding to the effective temperature of the standard star, to yield the final spectra. The spectra presented here are for the CBe stars HD 10516, HD 12856, HD 19243, HD 35345, β Mon A and β Mon C which were observed on 2009 November 8, 2010 December 12, 2009 November 7, 2010 December 13, 2010 October 22 and 2010 October 22 respectively. The corresponding standard stars used were SAO 22696, SAO 22859, SAO 12438, SAO 57819, SAO 151911 and SAO 151911. The spectral data reduction and analysis were done using IRAF tasks. In this work, we have presented the J band spectra of a few field CBe stars which have been observed as part of an ongoing program to study the J band spectra of CBe stars. A detailed analysis of the J band spectra of CBe stars will be presented later.

3. Results

In the optical, the focus was on studying the strengths of the OI 7774 and 8446 Å lines for reasons outlined below. To study the effects of the H Ly β /OI PAR process, KB95 have concentrated on five visible/infrared lines most relevant to the process. These are the forbidden line at 6300 Å which serves as a non-fluorescent standard when the line is available, the allowed 8446 Å transition which is an expected fluorescent product, the allowed multiplet at 7774 Å conventionally, thought to be independent of the H Ly β /OI PAR process, the allowed transition at 11287 Å which is the primary cascade line in the PAR process and an additional IR line at 11298 Å. The 6300 Å line is a suitable line of choice for examining effects of the PAR process in novae since it is seen in their spectra. However this line is hardly seen in our CBe spectra except in few and isolated cases where it is extremely weak; it is hence not a suitable diagnostic line for our purpose. On the other hand the 7774, 8846 Å lines are prominently seen in CBe star spectra and, as emphasized by KB95, their wavelength proximity introduces minimal errors when their strengths are compared even if the line intensities are not dereddened. We have also used the 11287, 13165 Å near-IR J band lines since the ratio of their line strengths is an effective discriminator between Ly β and continuum fluorescence as described in Grandi (1975) and Strittmatter et al. (1977). We note that a comprehensive J band spectral study of Be stars is unavailable though the $H\&K$ bands are well investigated (Clark & Steele (2000), Steele & Clark (2001)) as well as the L band (Granada, Arias & Cidale 2010). For that matter, the J band spectra of even isolated CBe stars are not readily encountered in the literature.

In the present study, CBe stars are broadly classified into three groups based on the

nature of OI 7774 and 8446 Å line profiles. Group I comprises of 83 stars which show both the OI 7774 and 8446 Å lines in emission (Figure 1, for a few examples). Out of these 83, 6 stars show the OI lines very weakly in emission making it difficult to measure the equivalent widths with any accuracy. Therefore we have omitted these stars and considered only 77 stars in Group I for the present analysis. Group II show OI 8446 Å in emission and 7774 Å in absorption with 26 CBe stars belonging to this category (top panel of Figure 2). Group III mostly includes objects (23 CBe stars) in which OI 8446 Å is in emission but 7774 Å is not prominent enough for a clear-cut classification, with the spectra we have, into a absorption or emission group (bottom panel of Figure 2). For comparing strengths of the 7774 and 8446 Å lines, it is meaningful to use only objects where both lines are in emission; we have thus restricted the analysis described below to objects from the first group.

3.1. Correction for measured OI equivalent widths

To estimate the equivalent width of OI λ 8446, it is necessary to deblend this line from Paschen 18 (P18, 8437 Å). It is possible to estimate the value of $W(\text{P18})$ by linearly interpolating between measured equivalent widths of the flanking lines P17 (8467 Å) and P19 (8413 Å) since the emission monotonically decreases along the Paschen series in this region as indicated by Briot (1981a) and Briot (1981b). This value of $W(\text{P18})$ may then be subtracted from the combined equivalent width of $W(8446 + \text{P18})$ to get the intrinsic value of $W(8446)$ in emission. To confirm the validity of this procedure we have plotted in Figure 3 the ratio of the mean equivalent widths of P14, P17, P19, P20, P21 normalized to the equivalent width of P17. In this figure we do not include P15 and P16 because they are blended with the CaII lines at 8542 and 8498 Å. The mean equivalent widths of the Paschen lines were computed from a sample of 26 stars which showed these lines the best and at a good signal to noise ratio. Such a selection enables us to measure the equivalent widths of these lines in a manner which is most reliable. The expected position of P18 (8437 Å) is shown by a dashed line. As may be seen from the Figure 3, the Paschen line strengths do show a monotonical increase with wavelength and then display a trend of flattening out around P17 and beyond. For our purpose of estimating the equivalent width of P18 it looks reasonable from the figure to approximate the value by interpolating between the equivalent width values of P17 and P19, individually for each star.

The flattening behavior of the Paschen line strengths beyond P17, shown in Figure 3, is possibly because these lines are optically thick and therefore being seen at a reduced intensity compared to that expected from recombination Case B analysis (Hummer & Storey (1987); Storey & Hummer (1995)). Similar behavior is seen for Brackett series lines (Steele & Clark

2001) and Humphrey and Pfund lines (Granada, Arias & Cidale 2010) which is attributed to optical depth effects.

Subsequent to the correction of $W(8446)$ from the contribution of P18, $W(7774)$ and $W(8446)$ are corrected for the underlying stellar absorption. This is necessary because these lines come into emission only after filling the underlying absorption component. The strength of this absorption component is estimated from the synthetic spectra of B0 —B9 main sequence stars of solar metallicity given by Munari et al. (2005) which are calculated from the SYNTHE code (Kurucz 1993) using NOVER models as the input stellar atmospheres (Castelli, Gratton & Kurucz 1997). We find W values of the components for the B0 to B9 classes respectively to be 0.006, 0.099, 0.143, 0.178, 0.209, 0.248, 0.272, 0.304, 0.345 and 0.400 Å respectively for the 7774 Å line and 0.003, 0.050, 0.074, 0.095, 0.111, 0.136, 0.153, 0.173, 0.199 and 0.236 for the 8446 Å line. These equivalent width values of the 7774 and 8446 Å absorption components are added to their corresponding emission values measured from the observed spectra to yield the final W values of the lines. The ratio of these equivalent widths is converted into a flux ratio by multiplying it with the ratio of continuum fluxes at 7774 and 8446 Å which is obtained from Kurucz (1992) models which are also given by Leitherer (<http://www.stsci.edu/science/starburst/Kurucz.html>). Typically the 7774/8446 continuum ratios from the Kurucz models are in the range 1.34 to 1.26 for B0 to B9 and closely match the 7774/8446 continuum ratio expected of a blackbody having an effective temperature of the corresponding B type star’s spectral class.

The derived line flux ratio is finally corrected for extinction where the extinction at 7774 and 8446 Å is derived from the parameterized, seventh order polynomial fit to the interstellar extinction given in Cardelli, Clayton & Mathis (1989). This gives $A(7774) = 0.6307A_V$ and $A(8446) = 0.5275A_V$ or equivalently $A(7774) - A(8446) = 0.32 \times E(B - V)$ with ratio of total-to-selective extinction, $R = 3.1$. The $E(B - V)$ values of the CBe stars are assumed to be equal to the mean $E(B - V)$ of the cluster with which it is associated. These values, available from the literature, are compiled in Mathew, Subramaniam & Bhatt (2008) and were used for extinction correction and are shown in column 9 of Table 1. However, it may be noted that the circumstellar envelope of a CBe star itself introduces an additional reddening expected to be of the order of $E(B - V) \sim 0.1$ magnitude (Dachs, Kiehling & Engels (1988); Slettebak (1985)). But this component is small compared to the cluster reddening (column 9, Table 1) and therefore should not significantly affect the dereddening corrections to the OI line flux ratio. The final dereddened line flux ratio $I(8446/7774)$, using the cluster $E(B - V)$ value, is given in column 10 of Table 1 and plotted in the right hand panel of Figure 4. In case we include the 0.1 mag additional reddening due to the circumstellar envelope then the $I(8446/7774)$ ratio is found to change very marginally by $\sim 3\%$.

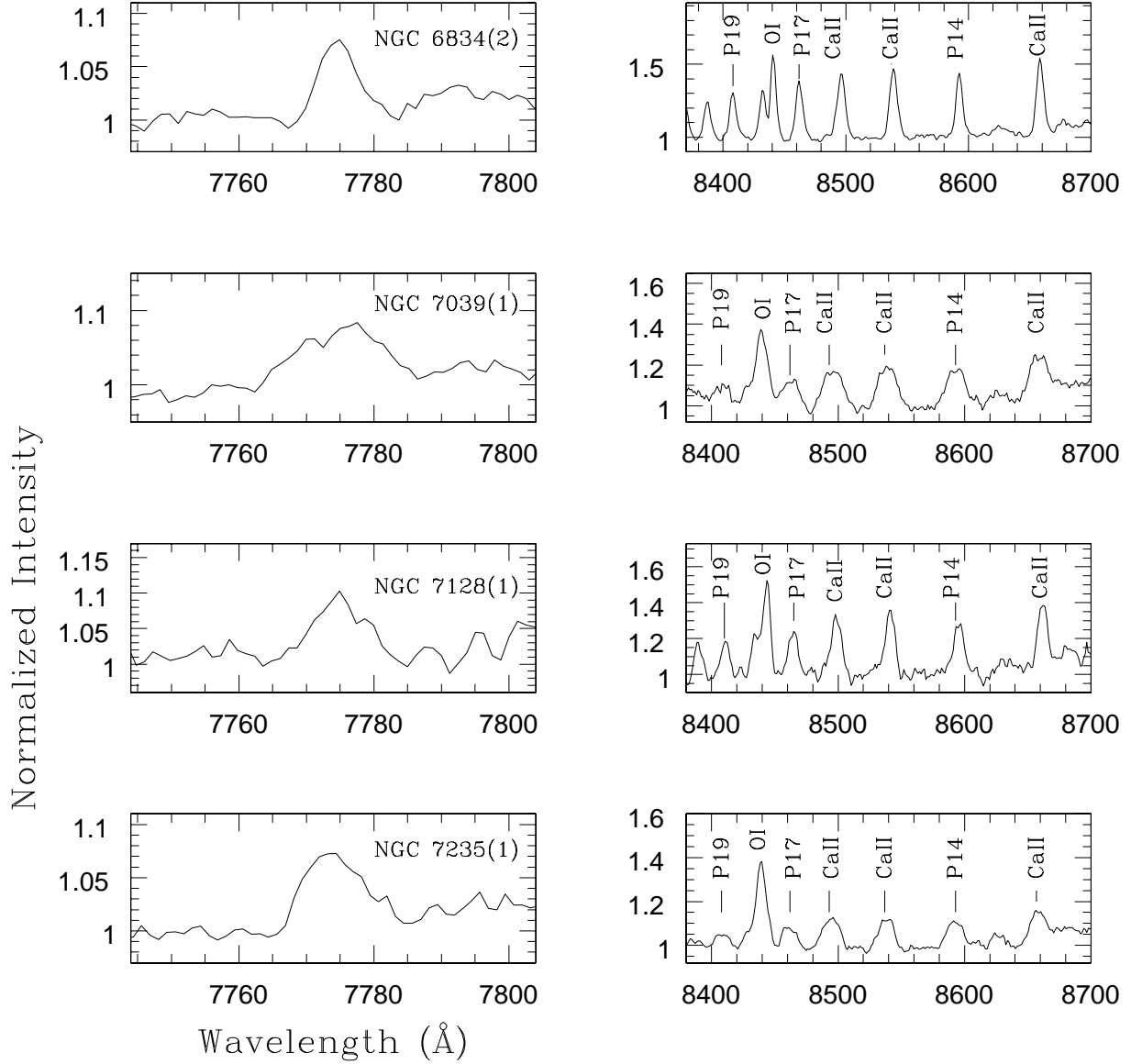


Fig. 1.— OI 7774 and 8446 line profiles of Group I candidates NGC 6834(2), NGC 7039(1), NGC 7128(1) and NGC 7235(1). Along with OI 8446 which is blended with Hydrogen Paschen 18 (P18), other lines seen are P14 8598 Å , P17 8467 Å , P19 8413 Å and CaII 8498, 8542, 8662 Å . The nomenclature of these CBe stars is given in Mathew & Subramaniam (2011)

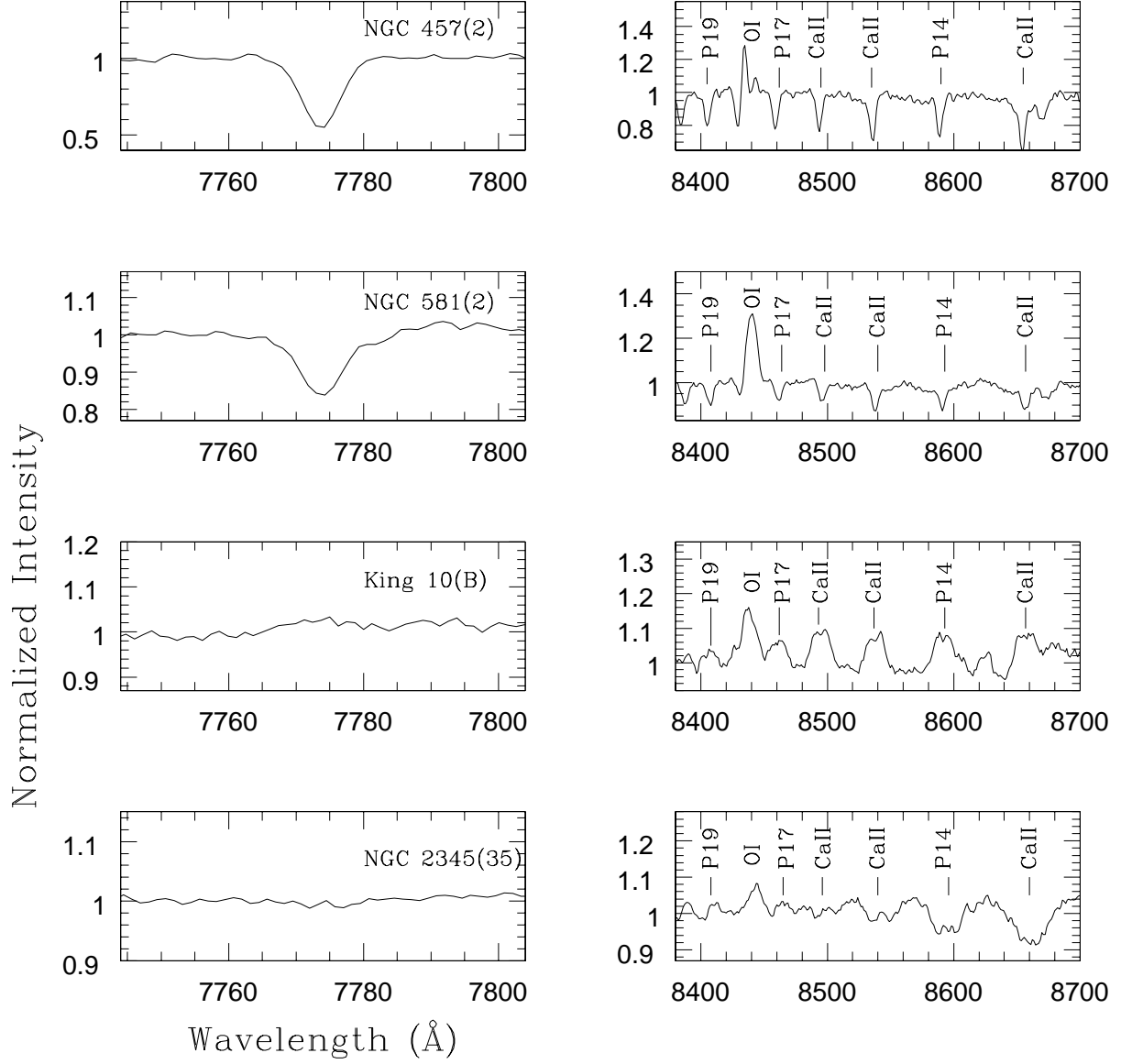


Fig. 2.— OI 7774 and 8446 line profiles of Group II candidates (1) NGC 457(2), (2) NGC 581(2) is shown in upper panel while that of Group III candidates (3) King 10(B), (4) NGC 2345(35) is shown in lower panel.

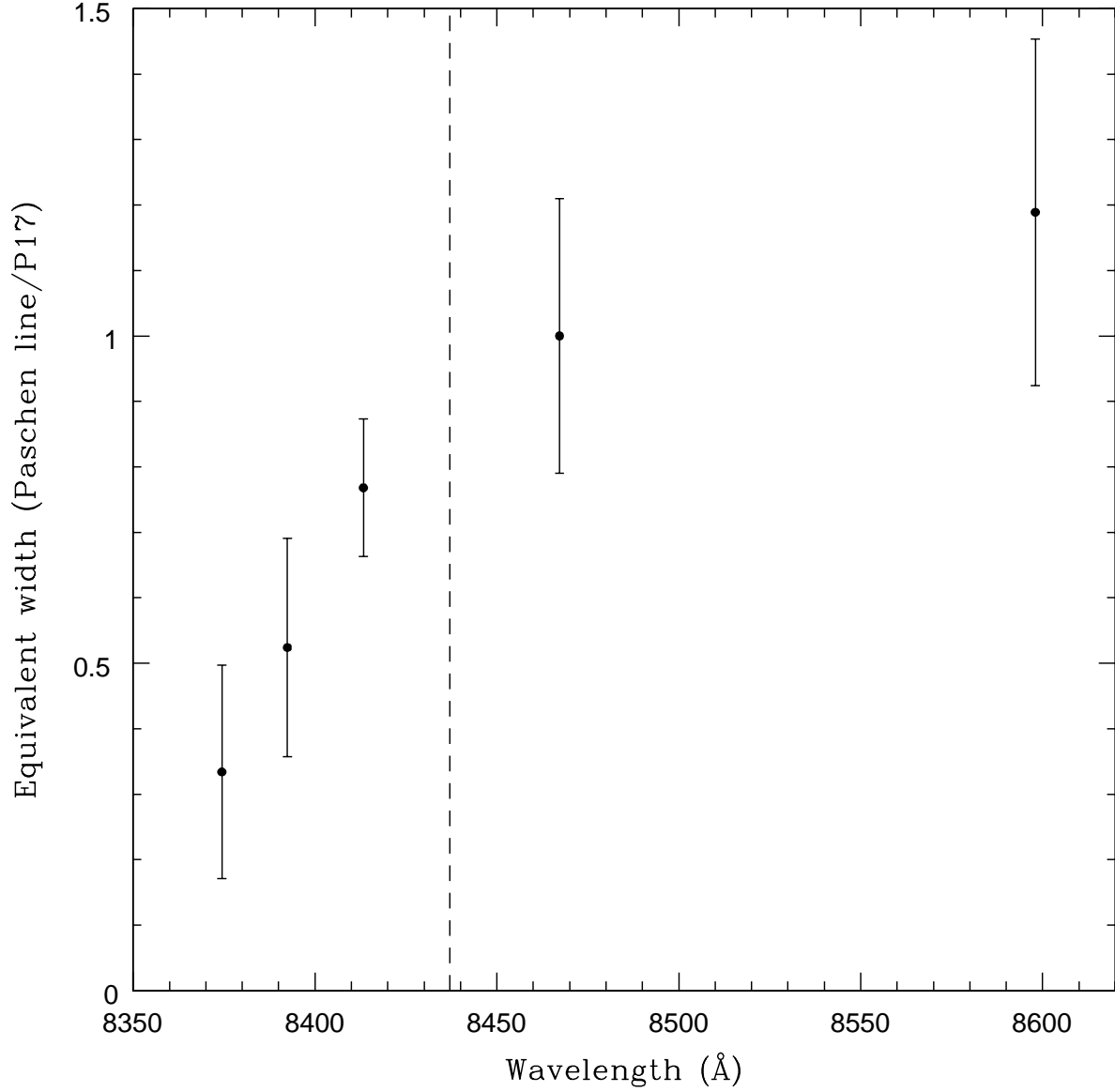


Fig. 3.— The ratio of the mean equivalent widths of the unblended Paschen lines P14, P17, P19, P20 and P21 normalized to the equivalent width of P17 is shown in the figure. The corresponding wavelengths of these lines are 8598, 8467, 8413, 8392 and 8374 Å respectively. The wavelength position of P18 (8437 Å) is shown in dashed line. Further details are given in the text in section 3.1.

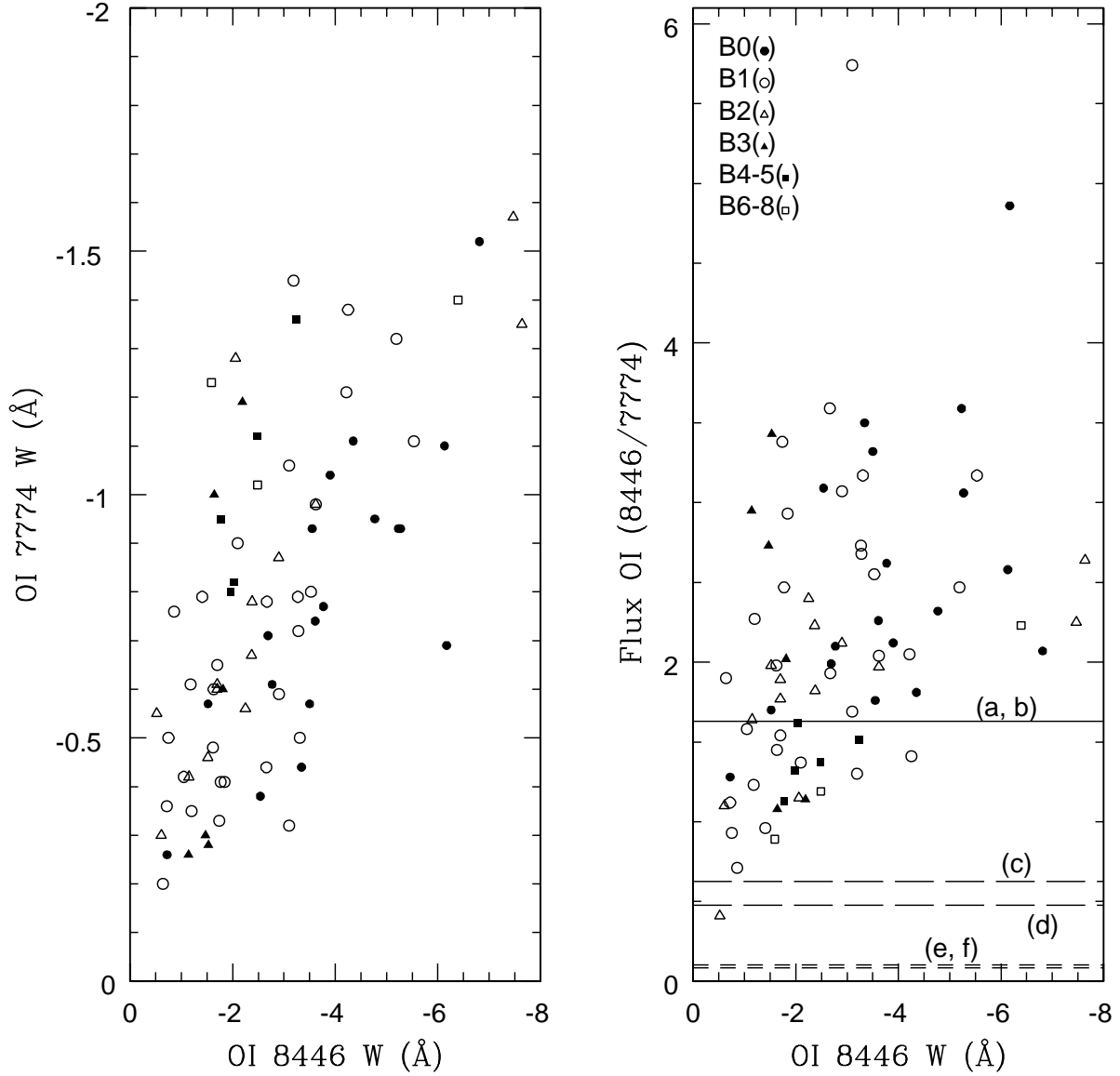


Fig. 4.— Plot between equivalent widths of the 7774 and 8446 Å lines for the sample of CBe stars is shown in the left panel. The flux ratio $I(8446/7774)$ is shown in right panel. Horizontal lines indicate the expected values of $I(8446/7774)$, from KB95, in the case of pure collisional excitation. The values are (a) 1.62 for $T = 10000$ K, $n_e = 10^{10} \text{ cm}^{-3}$, (b) 1.63 for $T = 20000$ K, $n_e = 10^{10} \text{ cm}^{-3}$, (c) 0.626 for $T = 10000$ K, $n_e = 10^{11} \text{ cm}^{-3}$, (d) 0.478 for $T = 20000$ K, $n_e = 10^{11} \text{ cm}^{-3}$, (e) 0.102 for $T = 10000$ K, $n_e = 10^{12} \text{ cm}^{-3}$ and (f) 0.083 for $T = 20000$ K, $n_e = 10^{12} \text{ cm}^{-3}$. The stars are binned based on their spectral types; B0 – filled circles, B1 – open circles, B2 – open triangles, B3 – filled triangles, B4 - B5 – filled squares and B6 - B8 – open squares.

3.2. Possibility of PAR process as the dominant excitation mechanism for OI emission lines in CBe stars

The expected $I(8446/7774)$ ratio from KB95, in the absence of the PAR process (i.e the parameter $R_p = -\infty$) is shown in Figure 4 (right hand panel) in straight lines. Essentially $R_p = -\infty$ represents the case of pure collisional excitation case of BK95. The $I(8446/7774)$ ratio is shown at two temperatures of 10000 K and 20000 K and three values of the electron density $n_e = 10^{10}$, 10^{11} and 10^{12} cm^{-3} . The choice of this parameter space for n_e and T , is a realistic approximation, of the actual range over which these parameters vary in Be star disk. There are several studies available in literature that model Be star disks in great detail to estimate disk parameters (e.g. Sigut & Jones (2007); Carciofi & Bjorkman (2008); Gies et al. (2007)). We find that a global view of disk parameters is offered by the work of Silaj et al. (2010) who generate and compare model and observed emission profiles for a statistically large sample of 57 CBe stars. These models use the code of Sigut & Jones (2007). The current models mentioned above assume that the disk density decreases, starting from a base density value of ρ_0 , with radial distance R as a power law with exponent n (that is $\rho \propto \rho_0(R_{star}/R)^n$). Silaj et al. (2010) point out that one of the interesting features of the derived disk density parameters is that a radial power-law index of $n = 3.5$ is strongly preferred for the model fits with 43% of the fits, over all stars considered, requiring this power-law index. We adopt this as a representative value for n . From their individually listed values of ρ_0 for the entire sample, we find a mean value of $1.09 \times 10^{-10} \text{ gm cm}^{-3}$ for ρ_0 equivalent to a density of $6.5 \times 10^{13} \text{ electrons cm}^{-3}$ assuming a completely ionized gas composed purely of Hydrogen. With $n = 3.5$ and a mean value of ρ_0 as above, and assuming a mean disk size of 6 to 8 R_{star} , the density ranges from 6.5×10^{13} at the inner edge to $\sim (0.5 \text{ to } 1.2) \times 10^{11} \text{ electrons cm}^{-3}$ at the outer edge of the disk. Thus a mean or representative value of n_e across the disk should be taken as $1 \times 10^{11} \text{ cm}^{-3}$ or greater; this is what we will adopt. The above models also show that the disk is not isothermal but the temperature of the matter in the disk is mostly seen to be in the range of 10000 to 20000 K.

Figure 4 (right panel) shows that for the adopted values of $n_e = 1 \times 10^{11} \text{ cm}^{-3}$ and $T = 10000$ to 20000 K, the $I(8446/7774)$ ratio of all stars barring one, lies above the value predicted from pure collisional excitation. This is also true for the case of $n_e = 10^{12} \text{ cm}^{-3}$ and, from the trend, should be true for higher densities too. The expected value of $I(8446/7774)$ for $n_e = 10^{10} \text{ cm}^{-3}$ is also shown, more to illustrate the dependence on n_e and T , but as argued before this is likely a lower than actual value for the electron density. Even in this case, a large number of stars show $I(8446/7774)$ to be significantly larger than expected. This shows that collisional excitation by itself cannot account for the higher than expected $I(8446/7774)$ ratio observed in Be stars and the PAR process, which enhances the strength of OI $\lambda 8446$, also contributes. In contrast, it may be mentioned that in the solar chromosphere

$I(8446/7774)$ is found equal to 0.2 ± 0.02 by Penn (1999) who therefore concludes that collisional excitation is more important than the PAR process in OI solar limb emission.

In Figure 4, the $I(8446/7774)$ strengths at densities of $n_e = 10^{10}$ and 10^{12} are from KB95. But since they have listed their data for increments in $\log n_e$ in steps of 2 (i.e $\log n_e = 4, 6, 8, 10$ and 12), the value of $I(8446/7774)$ at other intermediate densities such as $n_e = 10^9, 10^{11}$ etc were obtained from the authors by writing to them (Bhatia, private communication).

Although the density exponent $n = 3.5$ is favored by the Silaj et al. (2010) models, other values of the exponent could be considered too. But it may be noted that the bulk of their profiles, 84 percent to be precise, are modeled with $n \leq 3.5$. If we thus consider lower values of n , the density decline in the disk will be even slower in the disk compared to the $n = 3.5$ case. This will strengthen support for our arguments to consider a mean density in the disk of 10^{11} or more. An additional consideration may also be taken into account. Though interferometric data is now gradually emerging on emission zone size of lines like $H\alpha$ (e.g. Quirrenbach et al. (1997)) and a few other near-IR lines (e.g. Gies et al. (2007), Millan-Gabet et al. (2010)), no measurements are yet reported for the size of the OI line emitting region. But indirect estimates about the sizes of line emitting regions have been reported by Jaschek & Jaschek (1993) based on the observed velocity separation of the V (violet) and R (red) components of Be line profiles and the model by Huang (1972). Based on the entire Jaschek data we have derived the OI 8446 Å line emission region to have a mean size of 0.71 ± 0.27 of the $H\alpha$ emission region size. This implies that OI emission arises from relatively inner regions of the disk and therefore regions of higher density. Following Jaschek & Jaschek (1993) we estimate the radius of the $H\alpha$ emission region for the 10 CBe stars that showed double-peaked $H\alpha$ emission line profiles from the sample studied by Mathew & Subramaniam (2011). The mean value is around $12 R_s$ and $3.5 R_s$ for Keplerian and rigid body rotation for the particles in the disk. This translates to $8.5 R_s$ and $2.9 R_s$ for the size of OI 8446 emission region since OI 8446 line emission region is 0.71 times the $H\alpha$ emission radius, as derived earlier.

In Figure 4 we have also indicated the spectral class of the stars. Visual examination does not appear to indicate any significant correlation between the OI ratio and the spectral class. It may be expected that the temperature of the central star, which is essentially a measure of the spectral class, could affect the strength of the OI 8446 line via the amount of Lyman β radiation that the star emits. Eventhough this result looks promising, it needs to be strengthened further from the analysis of a large sample of CBe stars, especially late-type CBe stars.

If $Ly\beta$ fluorescence is operational in CBe stars one would expect a correlation between the emission strength of $H\alpha$ and OI $\lambda 8446$ lines, since $H\alpha$ and $Ly\beta$ both depend

on the population of the third hydrogen level (Bowen 1947). Kitchin & Meadows (1970) and Andriolat, Jaschek & Jaschek (1988) have studied the correlation between the measured equivalent widths of $H\alpha$ and $O\text{I } \lambda 8446$ emission lines in CBe stars. With our simultaneous observations of $O\text{I } \lambda 8446$ and $H\alpha$, it is interesting to derive a relation between their emission line equivalent widths. The $W(H\alpha)$ values for this analysis are for the same sample of stars analysed here but whose equivalent width values are reported in Mathew & Subramaniam (2011) while $W(8446)$ values are given in Table 1. From a simple linear fit, we have derived the following relation between $W(H\alpha)$ and $W(8446)$, both measured in \AA , for Group I stars as :

$$W(8446) = 0.10 \times W(H\alpha) + 0.53 \quad (1)$$

It is unlikely that recombination plays a dominant role in $O\text{I}$ excitation since the $I(8446/7774)$ ratio, in the case of recombination, should be around 0.6 as indicated by Grandi (1975, 1980) and Strittmatter et al. (1977). However, this is not the case here with the 8446 \AA line being stronger than the 7774 \AA line in most cases contrary to expectations. An interesting example where the $I(8446/7774)$ ratio becomes large due to the absence of recombination is in the Weigelt blobs around the LBV η Carinae. As proposed by Johansson & Letokhov (2005), the front of the blobs are ionized providing the Lyman β flux for the PAR process while the inner and distal regions of the blobs remain neutral because the ionizing flux cannot penetrate deep into the blobs. As a result recombination does not occur while the PAR process dominates leading to the extreme case of strong 8446 \AA emission being seen while the 7774 \AA line is completely absent.

Whether continuum fluorescence is the main source of excitation or not can be strongly constrained based on the ratio of strengths of the near-IR 11287 and 13165 \AA lines. It is expected that $W(13165)/W(11287) \geq 1$ if continuum fluorescence is the significant excitation mechanism (Strittmatter et al. (1977), Grandi (1975)). On the other hand, if the $\text{Ly}\beta$ fluorescence process dominates, the 11287 \AA line should become very strong as it is the primary line of the fluorescent cascade. The $W(13165)/W(11287)$ ratio is then expected to reverse and become smaller than unity. In novae, a large number of which have been studied by us in the near-IR (e.g. nova V1280 Sco – Das et al. (2008); nova V574 Puppis – Naik et al. (2010)), it is inevitably seen that $W(11287)$ is several times larger than $W(13165)$ strongly supporting the dominance of the PAR process in novae - analysis of other optical $O\text{I}$ lines independently establishes this (KB 95). An extreme case of a nova with extremely strong emission in the 11287 \AA line accompanied by no emission at 11365 \AA is V4643 Sgr (Ashok et al. 2006); nova V1500 Cygni also shows similar and extremely strong fluorescent lines of $O\text{I}$ (Strittmatter et al. 1977).

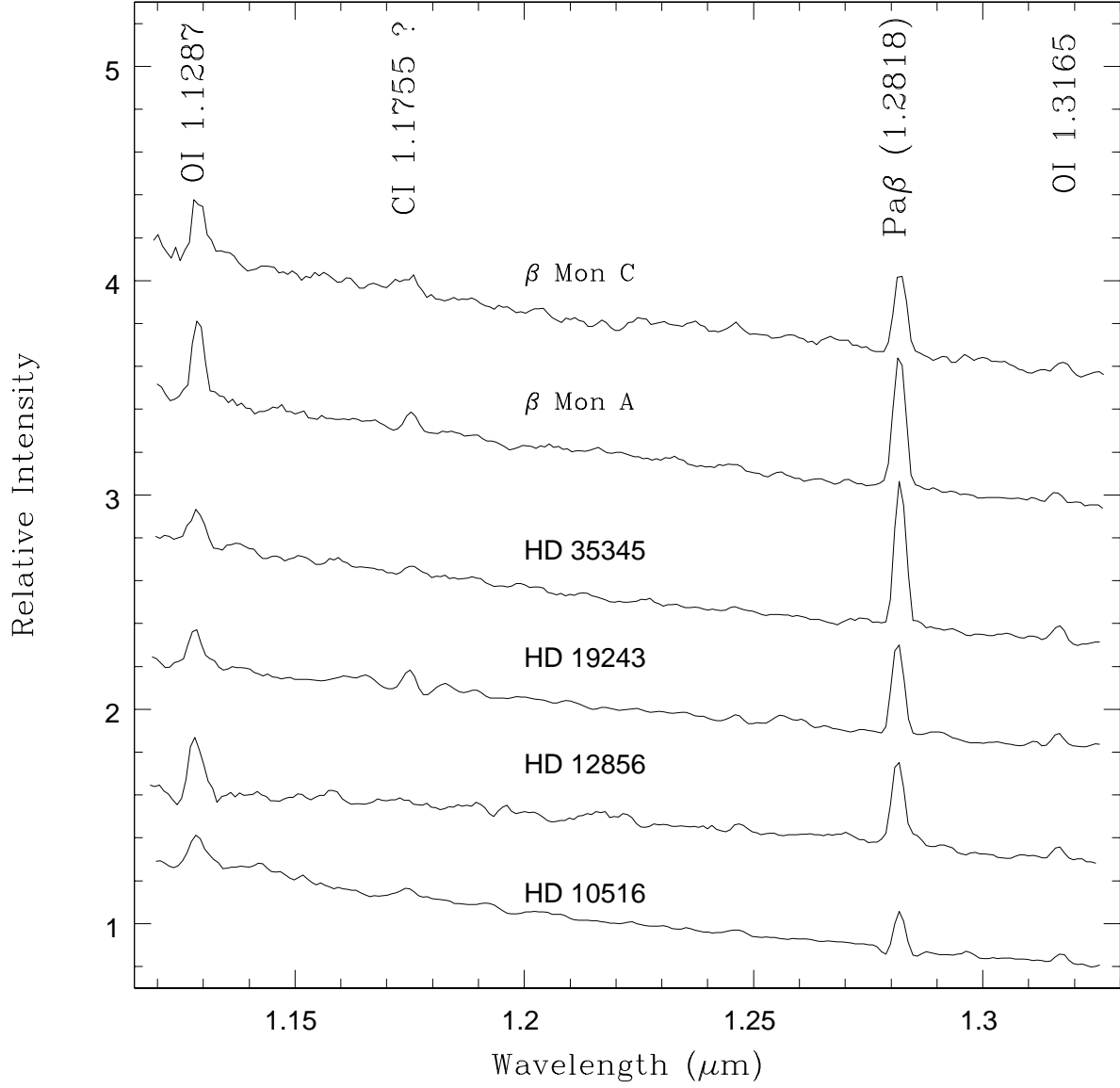


Fig. 5.— The J band spectra of selected CBe stars with the prominent lines identified. The spectra of the stars HD 10516, HD 12856, HD 19243, HD 35345, β Mon A, β Mon C are normalized with respect to the band center at 1.22 μm . There is offset between the adjacent spectra for clarity.

In Figure 5, we present the J band spectra of selected CBe stars from a larger sample studied by us to characterize their J band behavior (paper in preparation). It is found that whenever the 11287 and 13165 Å lines are present, as in the spectra shown, the former is always stronger of the two. This is seen in the spectra of Figure 5 where a mean value of $W(13165)/W(11287) = 0.30$ is found. Collisional excitation is also predicted to give $W(13165)/W(11287) \geq 1$ at $T = 10000$ and 20000 K respectively for $n_e = 10^{10} - 10^{12} \text{ cm}^{-3}$ (BK95). Thus both continuum fluorescence and collisional excitation are expected to make the 13165 Å line stronger than 11287 Å line. This is not seen and the $W(13165)/W(11287)$ ratio thus suggests that the $\text{Ly}\beta$ process has a significant role in exciting the near-IR lines in CBe stars. It may also be noted that continuum fluorescence if present, is expected to give significant contribution to the OI 7254 and 7002 Å lines (Strittmatter et al. 1977) and so also strong emission, comparable to OI 8446 Å, in the OI 7990 Å line (Netzer & Penston 1976). No traces of these OI lines are seen in our spectra within the detection limits (Mathew & Subramaniam 2011). Based on the above evidence and arguments in favor of the PAR process vis-a-vis other excitation mechanisms, we would conclude that the $\text{Ly}\beta$ fluorescence is operational in CBe stars.

We thank the referee for his suggestions and comments which helped in improving the manuscript. One of us (DPKB) thanks Dr. A. K. Bhatia for his help in providing additional computational data to us. The research work at Physical Research Laboratory is funded by the Department of Space, Government of India.

REFERENCES

- Andrillat, Y., Fehrenbach, Ch. 1982, A&AS, 48, 93
- Andrillat, Y., Jaschek, M., Jaschek, C. 1988, A&AS, 72, 129
- Ashok, N. M., Banerjee, D. P. K., Varricatt, W. P., Kamath, U. S. 2006, MNRAS, 368, 592
- Banerjee, D. P. K., Rawat, S. D., Janardhan, P. 2000, A&AS, 147, 229
- Bhatia, A. K., Kastner, S. O. 1995, ApJS, 96, 325
- Bowen, I. S. 1947, PASP, 59, 196
- Briot, D. 1981a, A&A, 103, 1
- Briot, D. 1981b, A&A, 103, 5

- Burbidge, E. M. 1952, *ApJ*, 115, 418
- Carciofi, A. C., Bjorkman, J. E. 2008, *ApJ*, 684, 1374
- Cardelli, J. A., Clayton, G. C., Mathis, J. S. 1989, *ApJ*, 345, 245
- Castelli, F., Gratton, R. G., Kurucz, R. L. 1997, *A&A*, 318, 841
- Clark, J. S., Steele, I. A. 2000, *A&AS*, 141, 65
- Collins, G. W. 1987, in *IAU Colloq. 92, Physics of Be Stars*, ed. A. Slettebak & T. P. Snow (Cambridge: Cambridge Univ. Press), 3
- Dachs, J., Hanuschik, R., Kaiser, D., Ballereau, D., Bouchet, P. 1986, *A&AS*, 63, 87
- Dachs, J., Kiehling, R., Engels, D. 1988, *A&A*, 194, 167
- Dachs, J., Hummel, W., Hanuschik, R. W. 1992, *A&AS*, 95, 437
- Das, R. K., Banerjee, D. P. K., Ashok, N. M., Chesneau, O. 2008, *MNRAS*, 391, 1874
- Gies, D. R. et al. 2007, *ApJ*, 654, 527
- Granada, A., Arias, M. L., Cidale, L. S. 2010, *AJ*, 139, 1983
- Grandi, S. A. 1975, *ApJ*, 196, 465
- Grandi, S. A. 1980, *ApJ*, 238, 10
- Hanuschik, R. W. 1986, *A&A*, 166, 185
- Hanuschik, R. W. 1987, *A&A*, 173, 299
- Huang, Su-Shu. 1972, *ApJ*, 171, 549
- Hummer, D. G., Storey, P. J. 1987, *MNRAS*, 224, 801
- Jaschek, C., Jaschek, M. 1993, *A&AS*, 97, 807
- Johansson, S., Letokhov, V. S. 2005, *MNRAS*, 364, 731
- Kastner, S. O., Bhatia, A. K. 1995, *ApJ*, 439, 346
- Kitchin, C. R., Meadows, A. J. 1970, *Ap&SS*, 8, 463
- Kurucz, R. L., 1992, in *IAU Symposium 149, The Stellar Populations of Galaxies*, ed. B. Barbuy & A. Renzini (Dordrecht:Kluwer), 225

- Kurucz, R., 1993, SYNTHE Spectrum Synthesis Programs and Line Data, CD-ROM No. 18
- Mathew, B., Subramaniam, A., Bhatt, B. C. 2008, MNRAS, 388, 1879
- Mathew, B., Subramaniam, A., 2011, BASI, 39, 517
- Meilland, A., Millour, F., Kanaan, S., Stee, Ph., Petrov, R., Hofmann, K.-H., Natta, A., Perraut, K. 2012, A&A, 538A, 110
- Millan-Gabet, R. et al. 2010, ApJ, 723, 544
- Munari U., Sordo R., Castelli F., Zwitter T. 2005, A&A, 442, 1127
- Naik, S., Banerjee, D. P. K., Ashok, N. M., Das, R. K. 2010, MNRAS, 404, 367
- Netzer, H., Penston, M. V. 1976, MNRAS, 174, 319
- Penn, M. J. 1999, ApJ, 518L, 131P
- Porter, J. M., Rivinius, T. 2003, PASP, 115, 1153
- Quirrenbach, A. et al. 1997, ApJ, 479, 477
- Sigut, T. A. A., Jones, C. E., 2007, ApJ, 668, 481
- Silaj, J., Jones, C. E., Tycner, C., Sigut, T. A. A., Smith, A. D. 2010, ApJS, 187, 228
- Slettebak, A. 1951, ApJ, 113, 436
- Slettebak, A. 1982, ApJS, 50, 55
- Slettebak, A. 1985, ApJS, 59, 769
- Steele, I. A., Clark, J. S. 2001, A&A, 371, 643
- Storey, P. J., Hummer, D. G. 1995, MNRAS, 272, 41
- Strittmatter, P. A. et al. 1977, ApJ, 216, 23

Table 1. List of CBe stars which show OI 7774 and 8446 in emission are shown with equivalent width and line flux ratio estimates. The coordinates and details of CBe stars are given in Mathew & Subramaniam (2011)

Be star	Sp.type	Obs.date	$W(7774)^a$	$W(8446)^a$	$W(7774)^b$	$W(8446)^b$	$I(8446/7774)$	$E(B - V)$	I_C^c
Berkeley86(26)	B1V	27-06-2005	-0.31	-1.72	-0.41	-1.77	3.22	0.90	2.47
Berkeley87(3)	B2	08-10-2005	-0.41	-0.45	-0.55	-0.52	0.71	1.90	0.41
Berkeley87(4)	B0-1V	09-10-2005	-0.45	-3.29	-0.50	-3.31	4.98	1.53	3.17
Berkeley90(1)	B0V	28-08-2006	-0.76	-3.77	-0.77	-3.77	3.68	1.15	2.62
Collinder96(1)	B0-1V	21-11-2005	-0.36	-1.81	-0.41	-1.84	3.37	0.48	2.93
IC4996(1)	B3	15-07-2005	-0.10	-1.44	-0.28	-1.53	4.23	0.71	3.43
King10(A)	B1V	29-07-2005	-0.50	-1.58	-0.60	-1.63	2.03	1.13	1.45
King10(C)	B2V	30-07-2005	-0.16	-0.54	-0.30	-0.61	1.54	1.13	1.10
King10(E)	B3V	31-07-2005	-0.12	-1.38	-0.30	-1.47	3.81	1.13	2.73
NGC436(2)	B5-7V	10-01-2007	-0.96	-1.44	-1.23	-1.59	1.03	0.50	0.89
NGC436(5)	B3V	09-01-2007	-0.42	-1.72	-0.60	-1.81	2.34	0.50	2.02
NGC457(1)	B3V	29-09-2006	-0.08	-1.05	-0.26	-1.14	3.41	0.49	2.95
NGC581(1)	B2V	28-09-2006	-0.46	-1.63	-0.60	-1.70	2.15	0.44	1.89
NGC581(3)	B0-1V	28-09-2006	-0.30	-1.18	-0.35	-1.20	2.58	0.44	2.27
NGC654(2)	B0-1	29-09-2006	-1.01	-3.08	-1.06	-3.10	2.20	0.90	1.69
NGC659(1)	B2V	21-11-2005	-0.53	-2.30	-0.67	-2.37	2.68	0.63	2.23
NGC659(3)	B1V	21-11-2005	-0.40	-0.70	-0.50	-0.75	1.12	0.63	0.93
NGC663(1)	B5V	08-10-2005	-0.70	-1.64	-0.95	-1.78	1.43	0.80	1.13
NGC663(2)	B0-1V	07-10-2005	-0.39	-2.63	-0.44	-2.66	4.54	0.80	3.59
NGC663(4)	B1V	24-10-2005	-0.38	-1.57	-0.48	-1.62	2.51	0.80	1.98
NGC663(5)	B1V	22-11-2005	-1.34	-3.14	-1.44	-3.19	1.65	0.80	1.30
NGC663(9)	B1V	24-10-2005	-1.11	-4.17	-1.21	-4.22	2.60	0.80	2.05
NGC663(11)	B2V	09-10-2005	-0.42	-2.18	-0.56	-2.25	3.04	0.80	2.40
NGC663(12V)	B0-1V	21-11-2005	-0.27	-3.07	-0.32	-3.10	7.27	0.80	5.74
NGC663(15)	B1V	25-10-2005	-0.80	-2.05	-0.90	-2.10	1.74	0.80	1.37
NGC663(16)	B1V	25-10-2005	-0.55	-1.65	-0.65	-1.70	1.95	0.80	1.54
NGC663(P5)	B2V	14-10-2005	-0.64	-2.31	-0.78	-2.38	2.31	0.80	1.82
NGC663(P8)	B2V	14-10-2005	-0.32	-1.45	-0.46	-1.52	2.51	0.80	1.98
NGC663(P23)	B2V	25-10-2005	-0.28	-1.08	-0.42	-1.15	2.08	0.80	1.64
NGC663(P25)	B0-1V	22-11-2005	-0.15	-0.61	-0.20	-0.64	2.41	0.80	1.90
NGC869(1)	B0V	21-01-2006	-0.92	-5.23	-0.93	-5.23	4.23	0.56	3.59
NGC869(2)	B0-1V	20-01-2006	-0.56	-1.16	-0.61	-1.18	1.45	0.56	1.23
NGC869(5)	B1V	20-01-2006	-0.32	-1.00	-0.42	-1.05	1.86	0.56	1.58
NGC884(1)	B0-1V	22-01-2006	-0.71	-0.83	-0.76	-0.86	0.84	0.56	0.71
NGC884(2)	B0-1V	22-01-2006	-1.06	-5.50	-1.11	-5.53	3.74	0.56	3.17
NGC884(5)	B0V	28-09-2006	-0.56	-1.52	-0.57	-1.52	2.00	0.56	1.70
NGC957(1)	B0-1V	07-12-2005	-0.67	-3.26	-0.72	-3.28	3.43	0.84	2.68
NGC1220(1)	B5V	21-11-2005	-0.87	-2.34	-1.12	-2.48	1.68	0.70	1.37
NGC1893(1)	B1V	21-11-2005	-1.22	-5.14	-1.32	-5.19	2.93	0.58	2.47
NGC2345(27)	B3V	28-12-2007	-1.01	-2.10	-1.19	-2.19	1.43	0.77	1.14
NGC2345(59)	B3V	07-12-2005	-0.82	-1.55	-1.00	-1.64	1.27	0.54	1.08
NGC2345(X2)	B5V	15-12-2007	-0.57	-1.89	-0.82	-2.03	1.88	0.50	1.62
NGC2414(2)	B1V	07-12-2005	-0.23	-1.69	-0.33	-1.74	3.93	0.51	3.38
NGC2421(1)	B1V	21-01-2006	-0.69	-3.22	-0.79	-3.27	3.09	0.42	2.73
NGC6649(1)	B0V	09-06-2007	-0.70	-2.69	-0.71	-2.69	2.84	1.20	1.99
NGC6649(6)	B5V	10-06-2007	-0.55	-1.84	-0.80	-1.97	1.88	1.20	1.32

Table 1—Continued

Be star	Sp.type	Obs.date	$W(7774)^a$	$W(8446)^a$	$W(7774)^b$	$W(8446)^b$	$I(8446/7774)$	$E(B - V)$	I_C^c
NGC6649(7)	B2V	10-06-2007	-0.84	-3.55	-0.98	-3.62	2.80	1.20	1.97
NGC6834(1)	B5V	07-10-2005	-1.11	-3.10	-1.36	-3.23	1.81	0.61	1.51
NGC6834(2)	B1V	07-10-2005	-0.49	-2.85	-0.59	-2.90	3.67	0.61	3.07
NGC7039(1)	B1-3V	21-11-2005	-1.14	-1.99	-1.28	-2.06	1.22	0.19	1.15
NGC7128(1)	B1V	14-10-2005	-0.88	-3.57	-0.98	-3.62	2.76	1.03	2.04
NGC7235(1)	B0-1V	14-10-2005	-0.75	-3.51	-0.80	-3.53	3.32	0.90	2.55
NGC7261(1)	B0V	07-12-2005	-1.03	-3.90	-1.04	-3.90	2.82	0.97	2.12
NGC7261(2)	B1V	07-12-2005	-0.26	-0.67	-0.36	-0.72	1.49	0.97	1.12
NGC7261(3)	B0-1V	07-12-2005	-0.73	-2.65	-0.78	-2.67	2.57	0.97	1.93
NGC7380(2)	B1-3V	17-07-2006	-0.73	-2.83	-0.87	-2.90	2.53	0.60	2.12
NGC7380(3)	B1-3V	17-07-2006	-0.47	-1.63	-0.61	-1.70	2.11	0.60	1.77
NGC7419(A)	B0V	15-07-2005	-0.43	-3.34	-0.44	-3.34	5.70	1.65	3.50
NGC7419(B)	B0V	27-06-2005	-0.92	-3.55	-0.93	-3.55	2.87	1.65	1.76
NGC7419(D)	B1V	15-07-2005	-1.28	-4.20	-1.38	-4.25	2.30	1.65	1.41
NGC7419(E)	B6	31-07-2005	-1.13	-6.24	-1.40	-6.39	3.62	1.65	2.23
NGC7419(G)	B0V	08-08-2005	-1.10	-4.35	-1.11	-4.35	2.95	1.65	1.81
NGC7419(I)	B0V	15-07-2005	-0.60	-2.77	-0.61	-2.77	3.41	1.65	2.10
NGC7419(J)	B0V	08-08-2005	-0.25	-0.72	-0.26	-0.72	2.08	1.65	1.28
NGC7419(L)	B0V	15-07-2005	-0.73	-3.61	-0.74	-3.61	3.67	1.65	2.26
NGC7419(M)	B0V	08-08-2005	-0.37	-2.54	-0.38	-2.54	5.02	1.65	3.09
NGC7419(N)	B2.5	08-08-2005	-1.41	-7.39	-1.57	-7.47	3.66	1.65	2.25
NGC7419(O)	B8V	08-08-2005	-0.68	-2.29	-1.02	-2.49	1.94	1.65	1.19
NGC7419(Q)	B1-3V	08-08-2005	-1.21	-7.57	-1.35	-7.64	4.29	1.65	2.64
NGC7419(1)	B0V	07-10-2005	-0.94	-4.77	-0.95	-4.77	3.77	1.65	2.32
NGC7419(3)	B0V	08-08-2005	-1.51	-6.81	-1.52	-6.81	3.37	1.65	2.07
NGC7419(4)	B0V	07-10-2005	-0.16	-2.39	-0.17	-2.39	10.6	1.65	6.52
NGC7419(5)	B0V	07-10-2005	-1.09	-6.13	-1.10	-6.13	4.19	1.65	2.58
NGC7510(1A)	B0V	24-10-2005	-0.56	-3.50	-0.57	-3.50	4.62	1.12	3.32
NGC7510(1B)	B1V	12-10-2005	-0.69	-1.36	-0.79	-1.41	1.33	1.12	0.96
NGC7510(1C)	B0V	13-10-2005	-0.92	-5.27	-0.93	-5.27	4.26	1.12	3.06
Roslund4(2)	B0V	25-10-2005	-0.68	-6.17	-0.69	-6.17	6.72	1.10	4.86

^aObserved equivalent widths in Å.

^bEquivalent widths in Å corrected for underlying stellar absorption component.

^cThis column gives the extinction corrected line flux ratio of $I(8446/7774)$.